High-Brightness High-Order Harmonic Generation by Truncated Bessel Beams in the Sub-10-fs Regime

M. Nisoli,* E. Priori, G. Sansone, S. Stagira, G. Cerullo, and S. De Silvestri
Istituto Nazionale per la Fisica della Materia, Centro di Elettronica Quantistica e Strumentazione Elettronica–C.N.R., Dipartimento di Fisica, Politecnico, Milano, Italy

C. Altucci
Istituto Nazionale per la Fisica della Materia, Dipartimento di Chimica, Università della Basilicata, Potenza, Italy

R. Bruzzese and C. de Lisio
Istituto Nazionale per la Fisica della Materia, Dipartimento di Scienze Fisiche, Università di Napoli "Federico II," Napoli, Italy

P. Villoresi, L. Poletto, M. Pascolini, and G. Tondello
Istituto Nazionale per la Fisica della Materia, Laboratorio di Elettronica Quantistica–D.E.I., Università di Padova, Padova, Italy
(Received 21 June 2001; published 2 January 2002)

Low-divergence, high-brightness harmonic emission has been generated by using a fundamental beam with a truncated Bessel intensity profile. Such a beam is directly obtained by using the hollow-fiber compression technique, which indeed allows one to optimize both temporal and spatial characteristics of the high-order harmonic generation process. This is particularly important for the applications of radiation, where extreme temporal resolution and high brightness are required.

DOI: 10.1103/PhysRevLett.88.033902 PACS numbers: 42.65.Ky, 42.50.Hz, 42.65.Re

When an intense short light pulse is focused into an atomic gas medium, extremely high harmonics of the incident-laser frequency can be generated [1–4]. High-order harmonic generation provides a tabletop source of coherent extreme ultraviolet (XUV) radiation, with pulse duration potentially in the subfemtosecond regime. The unique properties of the harmonic emission have opened the way to new applications in atomic and molecular spectroscopy, solid state and plasma physics, with a wide range of potential applications, such as plasma and material diagnostics, XUV nonlinear optics and attosecond physics. The optimization of the harmonic-generation conversion efficiency and of the spatial properties of the harmonic radiation are very important issues in such applications. Salières *et al.* [5,6] and Balcou *et al.* [7] have shown that, by using an excitation beam with Gaussian intensity profile, the conversion efficiency for harmonic generation strongly depends on the position of the nonlinear medium relative to the laser focus. In particular, the maximum efficiency is obtained when the medium is located just before the focus. For this position, the harmonic beam is completely annular with a large divergence, and therefore is characterized by low brightness. In order to generate high-order harmonics with good spatial properties, the medium must be located sufficiently after the laser focus, where the conversion efficiency is lower.

In this Letter we show, for the first time at our knowledge, that the use of a fundamental beam with a truncated-Bessel intensity profile, produced by propagation in a hollow fiber, allows one to significantly improve the spatial properties of the high-order harmonic beam. Since the hollow-fiber compression technique allows generation of few-optical-cycle pulses, this result is of particular relevance for applications of the XUV radiation, where extreme temporal resolution and high brightness are required. Thus far, the application of Bessel-Gauss beams to harmonic generation has been restricted to very low-order harmonics (third and fifth) [8–10].

In the experiments, the harmonic beam is produced by focusing sub-10-fs laser pulses into a neon jet. 25-fs pulses are coupled into an argon-filled hollow fiber [11,12], the spectrally broadened pulses are then compressed by chirped mirrors. Typical pulse duration ranges from 5 to 7 fs, and the spectral phase is nearly constant over the pulse spectrum [13]. By proper mode matching [14], the incident radiation can be dominantly coupled into the fundamental EH_{11} hybrid mode, whose intensity profile as a function of the radial coordinate, r, is given by $I(r) = I_0 J_0^2(2.405r/a)$ with $r \leq a$, where I_0 is the peak intensity, a is the capillary radius, and J_0 is the zeroth-order Bessel function of the first kind [15,16]. The sub-10-fs pulses are focused onto the gas jet by 25-cm focal length silver mirror. The laser-gas interaction length is $\sim$1 mm, with a gas pressure of $\sim$60 mbar. To observe the harmonic emission, we have used a high-resolution flat-field soft x-ray spectrometer and a high-resolution CCD detector, designed for the simultaneous acquisition of the spectrum and the far field pattern of the harmonic beam [17]. The spectrometer has been calibrated in order to provide an absolute measurement of the emitted photon flux.

We have performed measurements of the harmonic spatial profiles as a function of the nonlinear order and of the position of the gas jet relative to the laser focus. Hereafter, such relative position will be called z and will be

taken as positive when the laser beam is focused before the gas jet. Typical harmonic spectra obtained in neon for a laser peak intensity of $\sim 9 \times 10^{14}$ W/cm^2 at focus, are displayed in Fig. 1, for different z values. The horizontal axis is the spectral dispersion, going to longer wavelengths from the left to the right. The harmonic beam is characterized by regular spatial profiles, with small divergence even when the gas jet is located before and around the laser focus, without any evidence of annular profiles. The harmonic divergence continuously increases upon increasing the z value. This behavior is in contrast with previous measurements performed using longer pulses (135 fs) with different spatial characteristics [5,6]: In this case, when the gas jet was located close to the laser focus the harmonic angular distribution became increasingly distorted and eventually annular. The full width at half maximum (FWHM) of the harmonic angular distribution as a function of the nonlinear order, for different z values, is reported in Fig. 2. The spectrometer makes the projection of the two-dimensional profile of the harmonic beam in the direction perpendicular to the spectral dispersion. The minimum divergence is obtained when the laser is focused ~ 1 mm after the jet. Divergence increases with harmonic order in the plateau and slowly decreases in the cutoff region. Similar results have been obtained using helium as a nonlinear medium. The developed sub-10-fs-pulse-driven neon harmonic source emits $\sim 10^6$ photons/pulse per harmonic (in the plateau region), and within an estimated time interval of ~ 3 fs [18]. Figure 3 displays the brightness of the harmonic beam as a function of the position of the gas jet with respect to the focus, for two plateau harmonics (45th and 59th). The measured brightness per harmonic shows a maximum around $z = -1$ mm, given by $\sim 6 \times 10^{13}$ W/cm^2 srad (we have assumed a spot size of the emission area ranging from 13 to 25 μm for the different harmonic orders). It is worth pointing out that we have observed the same spatial characteristics using 25-fs driving pulses propagated along the hollow fiber without gas (in order to prevent spectral broadening). The reported measurements clearly demonstrate novel spatial properties of the harmonic emission: Regular harmonic spectral profiles, with small divergence, can be generated not only when the gas jet is located significantly after the laser focus, where conversion efficiency is not optimal, as previously observed, but in a considerably larger range of positions around the laser focus, including that corresponding to the maximum conversion efficiency. This result is particularly significant for applications where high XUV brightness is required.

We have then performed a theoretical study of the spatial properties of high-order harmonic radiation, using a nonadiabatic three-dimensional numerical propagation model [19,20] and the same parameters used in the experiments. The single-atom response is calculated using the strong-field model [21], generalized to account for nonadiabatic effects. As reported in Ref. [20], the numerical model can reproduce correctly the spectral characteristic of the harmonic beam. We have used the same numerical model to investigate the spatial properties of the harmonic beam.

By using in the calculation a fundamental beam with Gaussian intensity profile, we were unable to reproduce the experimental data. In particular, in this case the results

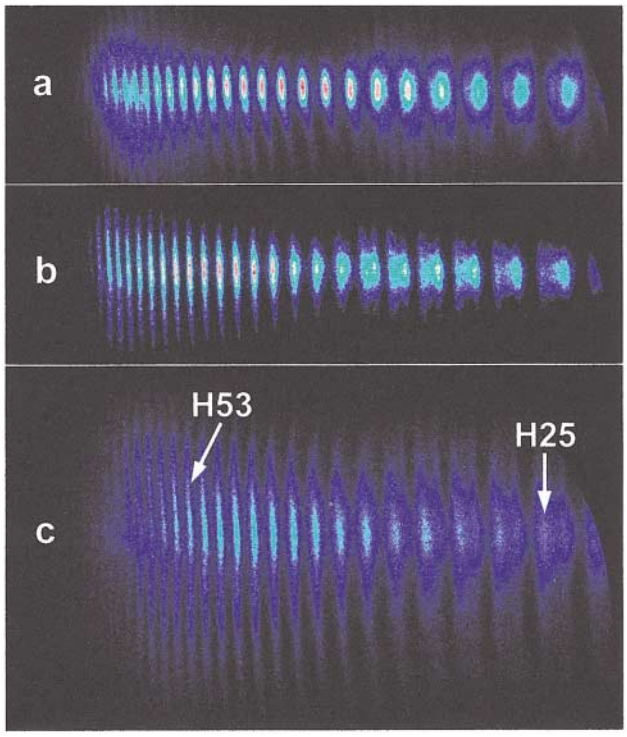

FIG. 1 (color). Harmonic spectra in neon generated by sub-10-fs pulses for three positions of the gas jet with respect to the laser focus: (a) $z = -1$ mm, (b) $z = 0$, (c) $z = 3$ mm. Vertical direction shows the spatial profile.

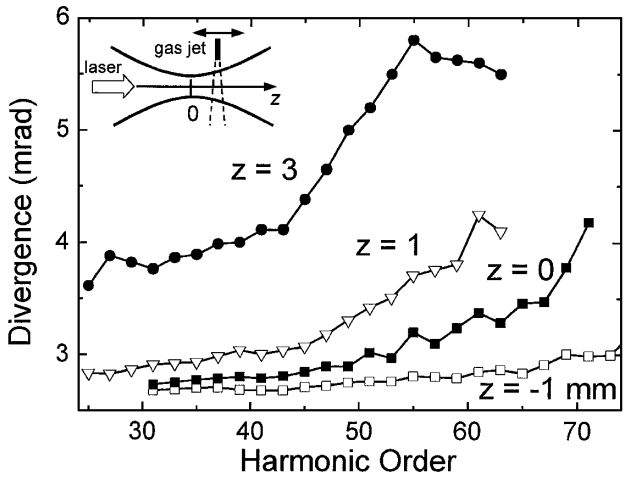

FIG. 2. Harmonic beam divergence vs harmonic order for various positions, z, of the gas jet with respect to the laser focus. The inset shows the interaction geometry.

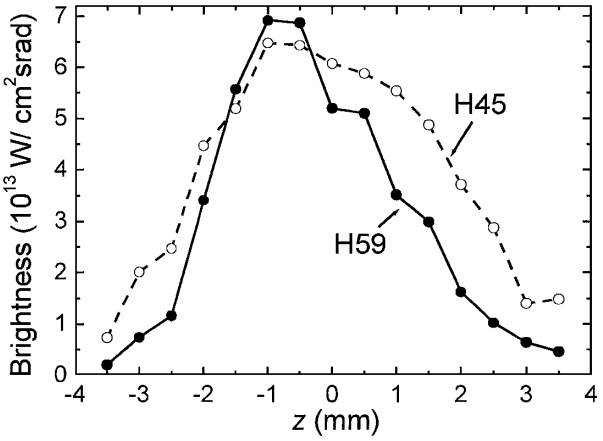

FIG. 3. Brightness of two harmonics (45th and 59th) vs position of the gas jet relative to laser focus.

of the calculation predict a harmonic divergence decreasing upon moving the gas jet away from laser focus in the propagation direction. Moreover, the spatial harmonic profile is narrow and regular only when the gas jet is placed well after focus ($z \geq 3$ mm). When the jet is moved near and before the focus, the profile becomes annular, as shown by the dashed line in Fig. 4(a), which presents the radial intensity profiles of the 45th harmonic for $z = 0$ in the case of the Gaussian excitation beam. These results are in agreement with previous calculations made by Salières *et al.* [5], in the case of longer driving pulses (150 fs), assumed to be Gaussian in space and time, but at odds with our experimental evidence. We have then performed simulations considering the actual spatial profile of the fundamental beam: a zeroth-order Bessel function truncated in correspondence of the first zero [15]. Figure 5 shows the FWHM of the harmonic angular distribution as a function of the harmonic order, for two different positions of the gas jet. The angular distributions have been calculated by integrating the two-dimensional profile of the harmonic beam over one direction, in order to reproduce the operation of the spectrometer. In this case, the numerical simulation presents a qualitative agreement with experimental data; in particular, the divergence correctly increases upon increasing the z value. The slight quantitative disagreement may be due to an unavoidable uncertainty of some experimental parameters (shape of the gas jet, gas pressure, etc.). Moreover, in agreement with the experimental results, the calculated harmonic beam displays regular spatial profiles even when the gas jet is moved near the laser focus, as shown by the solid lines in Figs. 4(a) and 4(b). When the gas jet is located well beyond the laser focus [$z \geq 3$ mm, see Fig. 4(b)], The profiles are of bell shape, irrespective of the order. On the other hand, when moving the jet around the laser focus [see Fig. 4(a)], the harmonic profile becomes very narrow, and does not display any annular structure. Upon increasing the nonlinear order, the profile presents narrow central peaks and long wings. It is important to note that the spectral characteristics of the harmonic beam are not significantly affected by the spatial profile of the fundamental beam.

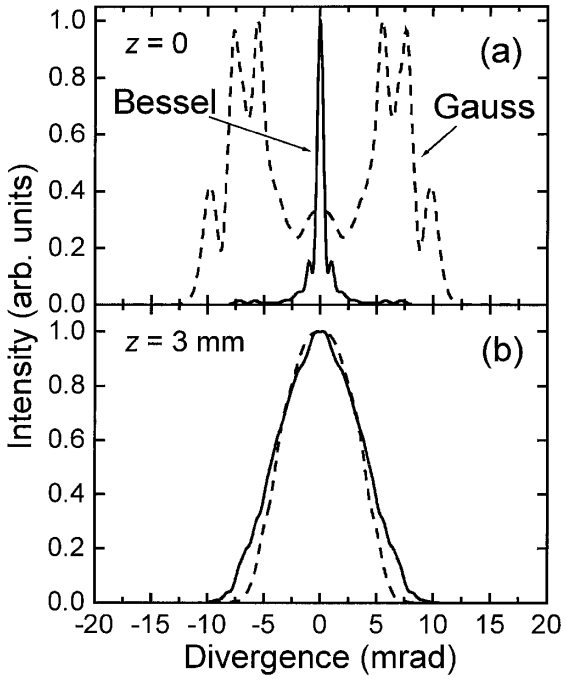

FIG. 4. Radial intensity profiles of 45th harmonic for (a) $z = 0$ and (b) $z = 3$ mm, calculated using the model described in the text, assuming a fundamental beam with Bessel (solid line) and Gaussian (dashed line) intensity profile.

To discriminate between the role of pulse duration and spatial characteristics of the fundamental beam, we have performed simulations using the analytical Lewenstein model [21], considering a continuous-wave monochromatic beam and neglecting ground-state depletion. The simulations show that, using a fundamental truncated-Bessel beam, the harmonics present a regular and collimated intensity profile, even when the gas jet is located before and around the laser focus, contrary to what

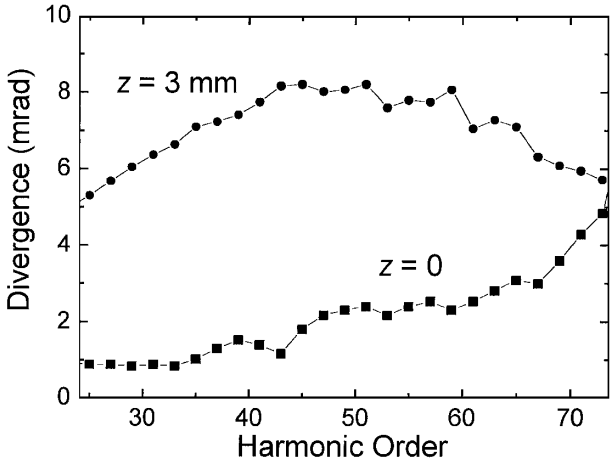

FIG. 5. Harmonic beam divergence vs harmonic order for various z positions, calculated using the model described in the text.

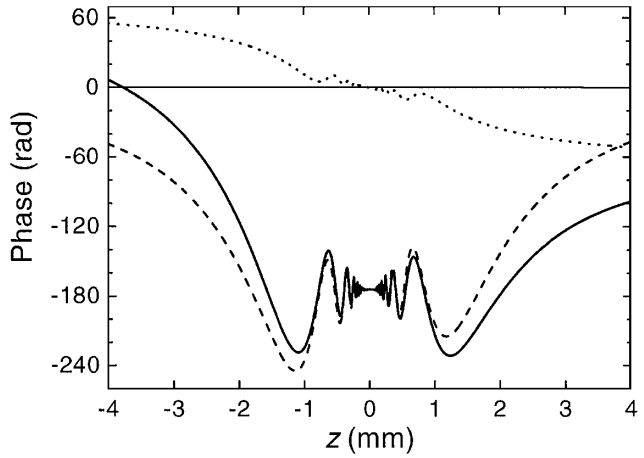

FIG. 6. Calculated phase of the nonlinear polarization on the propagation axis (solid line). The dashed line is the dipole phase for a peak intensity $I_0 = 9 \times 10^{14}$ W/cm^2; the dotted line is the phase term due to the propagation of the fundamental beam.

was obtained using a Gaussian excitation beam. Therefore, we can conclude that the improvement in the spatial characteristics of the harmonic radiation is essentially related to the use of a Bessel beam. A significant difference between a Gaussian and a truncated-Bessel beam, both focused by a spherical mirror, is that the latter shows an axial intensity, which, in the focal region, oscillates, with respect to the propagation coordinate, around an almost constant value. The extension of such oscillatory behavior is roughly equal to half of the confocal parameter of the best Gaussian fitting of the Bessel profile. The phase of the nonlinear polarization is the sum of two contributions: the dipole phase and a term due to the propagation of the fundamental beam. In the plateau, the dipole phase can be roughly approximated by $-5.8U_p/\omega$, where ω is the laser frequency and U_p is the ponderomotive energy [5]. The dipole phase depends on the z coordinate through the corresponding variation of the intensity of the fundamental beam, as displayed by the dashed line in Fig. 6, for a peak intensity $I_0 = 9 \times 10^{14}$ W/cm^2. As it is clearly shown in Fig. 6, due to the peculiar properties of a truncated-Bessel beam, the polarization phase on the propagation axis (solid line in Fig. 6) presents an oscillatory behavior around an almost constant value, in a $\sim$2-mm-wide region across the laser focus. We propose that such phase oscillations, which lead to a series of stationary phase points, provide a novel phase-matching mechanism, which favors the on-axis harmonic emission when the gas jet is located near the focus. On the other hand, when the nonlinear medium is placed well beyond the focus, the calculated polarization phase is similar to that obtained considering a Gaussian fundamental beam, and a good phase-matching condition on-axis is obtained [5].

In conclusion, we have shown that the angular distribution of high-order harmonics strongly depends on the spatial properties of the fundamental beam. The use of fundamental beams with a Bessel intensity profile allows significant improvements of the spatial quality of the harmonic beam. The hollow-fiber pulse compression technique, which allows one to directly obtain a Bessel intensity profile, thus provides an efficient tool to optimize both temporal and spatial characteristics of the high-order harmonic generation process. This is of special concern in the application of the XUV emission in various experiments, where extreme temporal resolution and high brightness are required.

This study was partially supported by the European Community's Human Potential Programme under Contract No. HPRN-CT-2000-00133, ATTO, and by the Istituto Nazionale per la Fisica della Materia under the project "Femtosecond Soft-X-Ray Generation by High Energy Laser Pulses."

*Email address: mauro.nisoli@fisi.polimi.it

[1] A. L'Huillier and Ph. Balcou, Phys. Rev. Lett. **70**, 774 (1993).
[2] J. J. Macklin, J. D. Kmetec, and C. L. Gordon III, Phys. Rev. Lett. **70**, 766 (1993).
[3] Ch. Spielmann *et al.,* Science **278**, 661 (1997).
[4] Z. Chang *et al.,* Phys. Rev. Lett. **79**, 2967 (1997).
[5] P. Salières, A. L'Huillier, and M. Lewenstein, Phys. Rev. Lett. **74**, 3776 (1995).
[6] P. Salières *et al.,* J. Phys. B **29**, 4771 (1996).
[7] P. Balcou *et al.,* Phys. Rev. A **55**, 3204 (1997).
[8] C. Altucci *et al.,* J. Opt. Soc. Am. B **17**, 34 (2000).
[9] C. F. R. Caron and R. M. Potvliege, J. Opt. Soc. Am. B **15**, 1096 (1998).
[10] C. F. R. Caron and R. M. Potvliege, J. Opt. Soc. Am. B **16**, 1377 (1999).
[11] M. Nisoli, S. De Silvestri, and O. Svelto, Appl. Phys. Lett. **68**, 2793 (1996).
[12] M. Nisoli *et al.,* Opt. Lett. **22**, 522 (1997).
[13] G. Cerullo *et al.,* IEEE J. Sel. Top. Quantum Electron. **6**, 948 (2000).
[14] M. Nisoli *et al.,* IEEE J. Sel. Top. Quantum Electron. **4**, 414 (1998).
[15] E. A. J. Marcatili and R. A. Schmeltzer, Bell. Syst. Tech. J. **43**, 1783 (1964).
[16] M. Nisoli *et al.,* Appl. Phys. B **65**, 189 (1997).
[17] L. Poletto, G. Tondello, and P. Villoresi, Rev. Sci. Instrum. **72**, 2868 (2001).
[18] M. Schnürer *et al.,* Phys. Rev. Lett. **83**, 722 (1999).
[19] E. Priori *et al.,* Phys. Rev. A **61**, 63801 (2000).
[20] P. Villoresi *et al.,* Phys. Rev. Lett. **85**, 2494 (2000).
[21] M. Lewenstein *et al.,* Phys. Rev. A **49**, 2117 (1994).